APPLIED AND ENVIRONMENTAL MICROBIOLOGY, Sept. 2005, p. 5465–5475 Vol. 71, No. 9
0099-2240/05/$08.00+0 doi:10.1128/AEM.71.9.5465–5475.2005

Generation and Phenotypic Characterization of *Aspergillus nidulans* Methylisocitrate Lyase Deletion Mutants: Methylisocitrate Inhibits Growth and Conidiation

Matthias Brock*

University Hannover, Institute for Microbiology, Herrenhäuser Str. 2, 30419 Hannover, Germany

Received 10 January 2005/Accepted 22 February 2005

Propionate is a very abundant carbon source in soil, and many microorganisms are able to use this as the sole carbon source. Nevertheless, propionate not only serves as a carbon source for filamentous fungi but also acts as a preservative when added to glucose containing media. To solve this contradiction between carbon source and preservative effect, propionate metabolism of *Aspergillus nidulans* was studied and revealed the methylcitrate cycle as the responsible pathway. Methylisocitrate lyase is one of the key enzymes of that cycle. It catalyzes the cleavage of methylisocitrate into succinate and pyruvate and completes the α-oxidation of propionate. Previously, methylisocitrate lyase was shown to be highly specific for the substrate (2*R*,3*S*)-2-methylisocitrate. Here, the identification of the genomic sequence of the corresponding gene and the generation of deletion mutants is reported. Deletion mutants did not grow on propionate as sole carbon and energy source and were severely inhibited during growth on alternative carbon sources, when propionate was present. The strongest inhibitory effect was observed, when glycerol was the main carbon source, followed by glucose and acetate. In addition, asexual conidiation was strongly impaired in the presence of propionate. These effects might be caused by competitive inhibition of the NADP-dependent isocitrate dehydrogenase, because the K_i of (2*R*,3*S*)-2-methylisocitrate, the product of the methylcitrate cycle, on NADP-dependent isocitrate dehydrogenase was determined as 1.55 μM. Other isomers had no effect on enzymatic activity. Therefore, methylisocitrate was identified as a potential toxic compound for cellular metabolism.

Propionate is a common carbon source in soil (9) and can be metabolized by a variety of microorganisms. Aerobic metabolism of propionate generally starts with the activation of propionate to the corresponding coenzyme A (CoA) ester propionyl-CoA as summarized in reference 32. One of the major pathways is that of the coenzyme B_{12}-dependent methylmalonyl-CoA pathway leading to the citric acid cycle intermediate succinyl-CoA. The other main pathway is the α-oxidation of propionate to pyruvate via the methylcitrate cycle. This pathway is found in bacteria, as well as in fungi, and involves a condensation of propionyl-CoA and oxaloacetate to methylcitrate (7, 17, 32). This reaction is catalyzed by a cycle specific methylcitrate synthase. The next step is the dehydration of methylcitrate to methylaconitate via a specific methylcitrate dehydratase. The rehydration of methylaconitate to methylisocitrate was shown at least in *Escherichia coli* and *Salmonella enterica* serovar Typhimurium to be catalyzed by the citric acid cycle aconitase AcnB (8, 16). The last pathway-specific reaction, catalyzed by a methylisocitrate lyase, is the cleavage of methylisocitrate into pyruvate and succinate. Methylisocitrate lyases have been well characterized, especially from bacterial but also from fungal sources (6, 13, 14, 22, 27, 28). However, only one gene sequence coding for a fungal methylisocitrate lyase has been published. It was shown that the so-called nonfunctional isocitrate lyase 2 from *Saccharomyces cerevisiae* possesses methylisocitrate lyase activity (22). The protein sequence showed a high degree of similarity to isocitrate lyases from other sources but solely exhibited activity toward methylisocitrate. Extracts of cells, which carried a deletion of the *ICL2* gene, showed a drastic reduction of methylisocitrate lyase activity compared to the wild type, when grown at the carbon sources threonine or ethanol. Unfortunately, no growth experiments had been performed to study the effect of the mutation on growth in the presence of propionate. Due to the high sequence similarity of this methylisocitrate lyase to isocitrate lyases, it was not possible to predict whether other uncharacterized fungal proteins display isocitrate lyase or methylisocitrate lyase activity. Although the specific methylisocitrate lyase from *Aspergillus nidulans* was purified and characterized (6), it was difficult at that time to gain access to the genome database from *A. nidulans*. Therefore, it was not possible to identify the corresponding gene and to study the phenotype of a deletion mutant.

In the food and feed industry, propionate is commonly used as a preservative against molds. This is surprising because of the ability of filamentous fungi to use propionate as the sole carbon source. Nevertheless, cometabolism of glucose and propionate strongly affects the growth rate in a manner, which is strictly dependent on the amount of propionate present (5, 7). It has been shown that propionyl-CoA possesses a severe negative effect on the pyruvate dehydrogenase complex from various organisms (2, 3, 5, 24). Deletion of methylcitrate synthase led to an inability of *A. nidulans* to remove propionyl-CoA, causing a strong accumulation of this compound. Therefore, the negative effect of propionyl-CoA on growth could at least in part be explained by a blockage of the pyruvate dehydrogenase complex. In addition to the growth-inhibitory effect of

* Present address: Leibniz Institute for Natural Product Research and Infection Biology, Hans Knoell Institute, Beutenbergstr. 11a, D-07745 Jena, Germany. Phone (3641) 656815. Fax: (3641) 656825. E-mail: Matthias.brock@hki-Jena.de.

TABLE 1. *A. nidulans* strains used in this study[a]

Strain	Genotype	Source or reference
A26 (*mclA*$^+$)	*biA1*	Fungal Genetics Stock Center, Kansas City, KS
RMS011 (*mclA*$^+$)	*pabaA1 yA2 ΔargB::trpCΔB trpC801 veA1*	30
SMI45 (*mclA*$^+$)	*pabaA1 yA2 wA3 veA1*	M. Krüger, Marburg, Germany
SMBA9 (Δ*mclA*)	*pabaA1 yA2 ΔargB::trpCΔB ΔmclA::argB trpC801 veA1*	This study
SMBA10 (Δ*mclA*)	*pabaA1 yA2 ΔargB::trpCΔB ΔmclA::argB trpC801 veA1*	This study
SRF200 (*mclA*$^+$)	*pyrG89 ΔargB::trpCΔB pyroA4 veA1*	18

[a] Methylisocitrate lyase-positive strains A26 and RMS011 were used as controls for excretion of methylisocitrate, growth inhibition, and induction of NADP-dependent isocitrate dehydrogenase.

propionyl-CoA, it also disturbed formation of polyketides, most likely via competition of propionyl-CoA with the natural substrates acetyl- and malonyl-CoA for the respective binding sites (5, 7, 36, 37).

In the present study the main interest was the investigation of the phenotypic effects caused by the accumulation of methylisocitrate. Previously, it was shown that NADP-dependent isocitrate dehydrogenase from bovine heart mitochondria and rat liver cytosol is strongly inhibited by α-*threo*-methylisocitrate with a K_i of <1 μM (1, 25). NADP-dependent isocitrate dehydrogenase also exists in *A. nidulans*, and the cytosolic, peroxisomal, and mitochondrial enzymes are all produced from a single gene (31). The exact function of this enzyme has not yet been proven. However, a general function may be the shuttle of reducing equivalents between NADP in different cellular compartments, because the compartmental membranes are impermeable for pyrimidine nucleotides and other small molecules. There are good indications that the mitochondrial enzyme is involved in the NADPH-dependent synthesis of glutamate from α-ketoglutarate (23). The peroxisomal enzyme might provide NADPH for the degradation of unsaturated fatty acids and the cytoplasmic enzyme provides NADPH for anabolic processes and for the reduction of glutathione and thioredoxin (19, 31).

By creating a mutant with a deletion of the gene coding for methylisocitrate lyase, it was possible to study the effect of intracellularly generated methylisocitrate on growth and development with a focus on NADP-dependent isocitrate dehydrogenase.

MATERIALS AND METHODS

Identification and deletion of the methylisocitrate lyase coding region. The gene coding for methylisocitrate lyase was identified from N-terminal sequencing of the purified protein and a subsequent BLAST search against the *A. nidulans* genome as described in Results.

In all transformation steps for generation of the deletion construct, *E. coli* MRF' XL1-Blue (MBI Fermentas, St. Leon-Rot, Germany) was used. The coding region including 1,154 bp upstream of the ATG start codon and 1,415 bp downstream of the TGA stop codon was amplified by DyNAzyme EXT DNA polymerase (BioCat, Heidelberg, Germany). The oligonucleotides used were MICLup2Pst (5′-CTA CG**C TGC AG**G CAC TCA TGA AG-3′; the PstI restriction site is in boldface) and AnMICLnest_down (5′-GGC AAT TCA CCG TCA AGG AC-3′). As template DNA genomic DNA from *A. nidulans* RMS011 was used. The resulting PCR product was cloned into the PCR2.1 vector (Invitrogen, Karlsruhe, Germany). Positive clones were analyzed by PstI restriction, releasing a fragment of 4,452 bp, which contained the *mclA* gene, the whole upstream region, and 1,287 bp of the downstream region (which possessed an internal PstI restriction site). The fragment was subcloned into a previously PstI-restricted pUC19 vector (Invitrogen). In order to exclude the coding region from the construct and for introduction of a NotI restriction site, an inverse PCR on the vector was performed with a proofreading polymerase (Accuzyme polymerase; Bioline, Luckenwalde, Germany). Oligonucleotides were NotMICLup (5′-**CCG C**GT GGA GTA CTG GAA GG-3′; reads toward the upstream region) and NotMICLdown (5′-**CCG C**TT TGA TGT GAG CGT TCG-3′; reads toward the downstream region), which both contained a half NotI restriction site (indicated in boldface). The resulting PCR product was eluted from an agarose gel and phosphorylated with polynucleotide kinase as described by the manufacturer (New England Biolabs, Frankfurt, Germany). The phosphorylated product was self-ligated with T4 DNA ligase (NEB) and yielded a vector with a pUC19 backbone, 1,131-bp upstream region, and 1,269-bp downstream region, both regions separated by a newly generated NotI restriction site. In this NotI site the *argB* gene from vector pAlcArg (7) was subcloned, leading to the final deletion construct. The deletion part was removed from the pUC-backbone by PstI restriction and used for transformation of *A. nidulans* RMS011 (Table 1).

Transformation of *A. nidulans* was performed by standard methods (34). Genomic DNA was isolated by standard procedures and subjected to XbaI restriction. A digoxigenin-labeled probe was amplified by PCR with digoxigenin-11-dUTP in the nucleotide mix and oligonucleotides NotMICLdown (see above) and MICLdown (5′-CTG CAG GCC GGC CAA GG-3′). This probe was specific for the downstream region. A Southern blot was performed on the restricted DNA, and bands were detected after hybridization with alkaline phosphatase-linked anti-digoxigenin Fab fragments (Roche Diagnostics, Mannheim, Germany) by use of CDP*star* as described in the manufacturer's protocol (Roche Diagnostics).

Isolation of RNA, reverse transcription, and sequencing of cDNA. Strain A26 (Table 1) was grown for 40 h on minimal medium containing 10 mM glucose and 100 mM propionate. The mycelium was harvested and frozen in liquid nitrogen, and ca. 0.1 g was ground to a fine powder. For RNA extraction, the RNeasy Plant Minikit (QIAGEN, Hilden, Germany) was used. An aliquot of the RNA was used as a template for first-strand cDNA synthesis with the sequence specific oligonucleotide cDNAmicl_down (5′-CAT ACA TAC ATT CGA ACG CTC AC-3′) and SuperScript II reverse transcriptase as described in the manufacturer's protocol (Invitrogen). Second-strand synthesis and amplification of the cDNA was performed by use of DyNAzyme EXT DNA polymerase and the sequence specific oligonucleotides cDNAmicl_down and cDNAmicl_up (5′-CAG TAC TCC ACG CCA GAC-3′). The resulting PCR product was cloned into the pDrive cloning vector (QIAGEN) and sequenced from both strands by SeqLab (Göttingen, Germany).

Phenotypic characterization of methylisocitrate lyase mutants and sexual crossing. Growth experiments were performed as described earlier (5). Mutant strains were inoculated in replicate cultures, and mycelium was harvested after growth for the indicated time (result section). Carbon sources used for growth were glucose, sodium acetate, sodium propionate, and glycerol in the concentrations and combinations described for each experiment. For determination of growth inhibition, mycelium was harvested and dried for at least 12 h at 80°C and weighed. Biomass obtained from glucose, acetate, or glycerol as the sole carbon source was set as 100%, respectively.

The ability of the mutant strains to form conidia was determined from solid plates containing 2% agar and the indicated carbon sources. Spore suspensions were point inoculated, and plates were incubated for 3 days at 37°C (the growth time for plates containing propionate as sole carbon source was prolonged to 7 days).

Crossing of the yellow strain SMBA9 and the green strain SRF200, which carries an intact methylisocitrate lyase locus, was performed by standard procedures. In brief, both strains were inoculated on plates, which allowed both strains to grow. Agar blocks were removed from areas, where mycelium of both strains was found and transferred to an agar plate that lacked *p*-aminobenzoic acid and uracil. Only mycelium, which contained nuclei from both strains was able to grow on these plates. The plates were sealed and incubated for 10 days at 37°C, which

induced the formation of cleistothecia. Mature cleistothecia were isolated and plated on nonselective media. A successful crossing event was monitored by green and yellow colonies in a 1:1 deviation. Single colonies were analyzed for their phenotypes on selective media. Pictures of the colonies were taken with a digital camera (Nikon Coolpix 995).

Purification of isocitrate lyase. Isocitrate lyase from *A. nidulans* was purified from strain SMI45, which was grown for 40 h in minimal medium containing 100 mM acetate and 100 mM propionate as carbon sources. This composition of the medium induced both isocitrate lyase and methylisocitrate lyase activity (5). During the purification procedure fractions were checked for both activities.

Approximately 4 g of dry pressed mycelium was ground to a fine powder under liquid nitrogen and resuspended in 50 ml of buffer A (50 mM Tris-HCl, 2 mM $MgCl_2$, 2 mM dithiothreitol [pH 8.0]). Cell debris was removed by centrifugation at 25,000 × *g* at 4°C for 20 min. The supernatant was subjected to fractionated $(NH_4)_2SO_4$ precipitation from 0 to 40% and from 40 to 75% saturation. The pellet from the second precipitation was resolved in 5 ml of buffer A and loaded on a Phenyl-Sepharose column (bed size, 20 ml) previously equilibrated with buffer A containing 1 M $(NH_4)_2SO_4$. Proteins were eluted with a decreasing $(NH_4)_2SO_4$ gradient from 1 to 0 M. Isocitrate lyase containing fractions were pooled, concentrated, and desalted by use of centrifugal filter devices (30-kDa cutoff; Millipore, Schwalbach, Germany) and buffer A. The concentrated sample was loaded onto a ResourceQ column (bed size, 1 ml; Amersham Biosciences Europe, Freiburg, Germany) and eluted against a sodium chloride gradient from 0 to 0.2 M in buffer A. Enzyme-containing fractions were collected, desalted, and again subjected to chromatography on a ResourceQ column.

Purity of the active fractions was determined by sodium dodecyl sulfate-polyacrylamide gel electrophoresis (20). Further identification was made by peptide mass analysis. The purified protein band was excised from the gel and sent to the Ludwig-Maximilians-Universität München. The protein was digested with trypsin and peptides were subjected to matrix-assisted laser desorption ionization–time of flight analysis. The peptide masses were than compared to nonredundant protein databases.

Enzyme assays and determination of methylisocitrate from the growth medium. The activities of isocitrate lyase and methylisocitrate lyase were determined as described before (5). The K_m value of isocitrate lyase for the substrate D-isocitrate was identified by varying the substrate concentration of D,L-isocitrate in the assay from 1 to 0.1 mM, giving an effective substrate concentration of D-isocitrate in the range of 0.5 and 0.05 mM. The K_m value for (2*R*,3*S*)-2-methylisocitrate was determined with stereoisomeric pure substrate (10) in a range of 1.5 and 0.25 mM.

Methylisocitrate lyase activity in mutant strains was defined with 0.5 mM methylisocitrate in the assay, which would have been sufficient for maximum activity of methylisocitrate lyase (K_m = 31 μM) (6).

The concentration of methylisocitrate in the growth medium was tested by enzymatic methods after harvest of the mycelium. Samples of 50 to 100 μl were applied to a test containing NADH and lactate dehydrogenase. The assay was started by the addition of purified methylisocitrate lyase from *E. coli*, and the decrease in absorbance at 340 nm was monitored. Concentrations of methylisocitrate from the complete culture broth were calculated and referred to the mycelial dry weight.

NADP-dependent isocitrate dehydrogenase was assayed by monitoring the formation of NADPH in a slightly modified procedure as described in reference 1. The final assay with a volume of 1 ml contained: 50 mM Na-HEPES (pH 7.5), 2 mM D,L-isocitrate, 1 mM $MnCl_2$ (or 2 mM $MgCl_2$), 1 mM NADP, and crude extract. For determination of the K_m value, all components were kept constant except the concentration of isocitrate, which was used in an effective concentration (D-isocitrate) between 1.0 and 0.025 mM. The inhibition constant of methylisocitrate was determined by preincubating the respective assay mixture with 25, 50, or 100 μM (2*R*,3*S*)-2-methylisocitrate and starting the reaction with an effective concentration of D-isocitrate in the range of 1.5 and 0.375 mM. The K_i was calculated from the factor of the increase of the K_m with respect to the inhibitor concentration used.

Protein concentrations were determined by use of Bio-Rad protein assay concentrate (Bio-Rad Laboratories, Munich, Germany) as described in the manufacturer's protocol with bovine serum albumin as a standard.

RESULTS

Identification of the gene coding for methylisocitrate lyase. Methylisocitrate lyase was purified from *A. nidulans* wild type as described in an earlier publication (6). After blotting of the purified enzyme on a polyvinylidene difluoride membrane (Millipore), the purified enzyme was subjected to N-terminal sequencing (kindly carried out by D. Linder, Justus-Liebig-University, Giessen, Germany) and revealed the putative peptide sequence SPSSLPPVQPP.

The exact interpretation of the sequence data was difficult because of the high amount of proline, which weakens the signal and leads to a high background. Nevertheless, a BLAST search against fungal proteins (http://www.ncbi.nlm.nih.gov/BLAST/) revealed a single hit on the hypothetical protein AN8755.2 (accession no. EAA60548) from the annotated *A. nidulans* genome (http://www.broad.mit.edu/annotation/fungi/aspergillus/index.html). Sequencing of the cDNA obtained with specific oligonucleotides confirmed the predicted sequence with an exception at the C-terminal end (accession no. AJ890109; protein ID no. CAI65406). At this site the sequence of the hypothetical protein is extended by 10 amino acids, which is mainly due to a wrong intron prediction at the C-terminal end. The protein consists of 604 amino acids with a molecular mass of 66.9 kDa, which is in good agreement with 66 ± 3 kDa as determined from sodium dodecyl sulfate-polyacrylamide gel electrophoresis (6). However, a mitochondrial localization of the native enzyme was predicted because that seems to be the compartment in which the methylcitrate cycle takes place (7, 22). Therefore, the protein was scanned for a putative mitochondrial targeting sequence with the program MITOPROT (http://ihg.gsf.de/ihg/mitoprot.html). With a probability of 0.9992 (maximum = 1.0) the protein is transported to mitochondria with a cleavage site of the leader peptide at position 41 (MLRSIPRRVPRRLPIFTTTATAGGPSR LAQRAFTCGYLRM/SPSSL. . .), which is in perfect agreement with the result from N-terminal sequencing. The native protein therefore has a molecular subunit size of 62.4 kDa, which is also consistent with that determined from gel electrophoresis.

The corresponding gene is located at the right arm of chromosome III and spans a region of 2,081 nucleotides (including five introns) on contig 1.161 (positions 60367 to 62448).

Prediction of a conserved sequence motif for fungal methylisocitrate lyases. In previous publications, the crystal structure of isocitrate lyases from *Mycobacterium tuberculosis* (26) and from *A. nidulans* (4) had been determined. In addition, the structure of bacterial methylisocitrate lyases from *E. coli* and *Salmonella enterica* serovar Typhimurium had also been determined (14, 28). Interestingly, the sequence identity of the *E. coli* methylisocitrate lyase (PrpB) to the respective isocitrate lyase (AceA) was only 27%, but the structural identity was extremely high. Furthermore, a high sequence identity was found within the amino acids of the active site.

Isocitrate lyases contain conserved tryptophan, phenylalanine, and threonine residues, which are responsible for correct orientation of the glyoxylate moiety in the active site. In contrast, in bacterial methylisocitrate lyases the amino acids phenylalanine, leucine, and proline replaced these residues. Modeling of pyruvate into the active site revealed that these exchanges lead to a hydrophobic binding pocket, which gives more space for the additional methyl group of pyruvate (14).

An alignment of the methylisocitrate lyase from *S. cerevisiae* (ICL2) revealed that the first tryptophan residue from isocitrate lyases was still conserved but that phenylalanine and threonine were replaced by leucine and serine. Both changes may also provide more space for an additional methyl group. To

```
AnMICL  452  FGPYADLLWVETGDP.....DEASLKSFIWDLAQHGFVLQLISLAGLH 530
NcMICL  465  FGPYADLLWVETGDP.....TQDTLKSFVWDIAKEGFTLQLVSLAGLH 543
MgMICL  454  FAPYADLLWVETGDP.....TEQTLKSFIWDIAKEGFVLQLVSLAGVH 532
ScMICL  421  FAPYSDMIWLETKTP.....DDKALKSFVWDLAKEGFTLQLVSLAGLH 499
YlMICL  413  FAPYADLIWLETKTP.....SDEQLKSFVWDLAKSGFVMQLISLAGLH 491
IclAn   385  YAPFADLIWMESKLP.....PRDEQETYIKRLGALGYAWQFITLAGLH 462
IclNc   396  YAPYCDAIWMESKLP.....GRDDQETYIRRLAKLGYCWQFITLAGLH 472
IclMg   395  YAPYADAIWMESKLP.....PRDEQETYIRRLAGLGYCWQFITLAGLH 472
IclSc   399  FAPYADLVWMESNYP.....SVDEQHTFIQRLGDLGYIWQFITLAGLH 476
ICLYl   385  YAPYADLIWMESKLP.....SPEDQETYISRLAKLGYVWQFITLAGLH 462
```

FIG. 1. Partial alignment of fungal methylisocitrate lyases and isocitrate lyases. Putative active site residues are shown in boldface. Residues, which may specify the acceptance of the methyl group from methylisocitrate are in boldface and shaded. AnMICL, methylisocitrate lyase from *A. nidulans* (accession no. CAI65406); NcMICL, hypothetical methylisocitrate lyase from *N. crassa* (accession no. XP_331680); MgMICL, hypothetical methylisocitrate lyase from *M. grisea* (accession no. EAA47373); ScMICL, methylisocitrate lyase from *S. cerevisiae* (accession no. NP_015331); YlMICL, hypothetical methylisocitrate lyase from *Y. lipolytica* (Accession: XP_506117); IclAn, isocitrate lyase from *A. nidulans* (accession no. EAA62727); IclNc, isocitrate lyase from *N. crassa* (accession no. CAA44573); IclMg, isocitrate lyase from *M. grisea* (accession no. AAN28719); IclSc, isocitrate lyase from *S. cerevisiae* (accession no. NP_010987); IclYl, isocitrate lyase from *Y. lipolytica* (accession no. XP_501923).

check whether this is a general motif of fungal methylisocitrate lyases, a BLAST search against fungal databases was performed using the sequences from *S. cerevisiae* and *A. nidulans* as a template. The hypothetical methylisocitrate lyases from *Neurospora crassa*, *Magnaporthe grisea*, and *Yarrowia lipolytica* were identified by similarity and by their putative mitochondrial targeting sequence. An alignment of the residues, which are proposed to be involved in substrate binding of these methylisocitrate lyases against their isocitrate lyase counterparts, is shown in Fig. 1.

From this sequence alignment we predict a sequence motif [GF(V/T)(L/M)Q**L**(I/V)**S**LAG(L/V)H; amino acids providing the space for the methyl group are indicated in boldface] to be specific for fungal methylisocitrate lyases.

Deletion of the methylisocitrate lyase coding region and identification of mutant strains. The coding region of the methylisocitrate lyase gene (*mclA*) with flanking regions was amplified from genomic DNA of strain RMS011 (Table 1). Thereby, a PstI restriction site ca. 1.15 kb upstream of the start ATG was introduced and, additionally, the endogenous PstI restriction site ca. 1.29 kb downstream of the stop codon was included. This enabled the subcloning into pUC19 vector. The coding region of the *mclA* gene was removed by PCR, generating a NotI restriction site in which the *argB* gene from *A. nidulans* (coding for carbamoyl transferase and leading to arginine prototrophy of transformants) was cloned. In this construct, a 1.13-kb upstream and a 1.27-kb downstream fragment of the *mclA* flanking regions surrounded the *argB* gene. For transformation of *A. nidulans* strain, RMS011 the vector backbone of the deletion construct was removed by PstI restriction, and only the deletion part was used further. Transformation of protoplasts was performed as described elsewhere (34). Genomic DNA from transformants was isolated, XbaI restricted, and subjected to Southern analysis using a digoxigenin-labeled probe against the downstream fragment. The wild type was supposed to yield a 1.8-kb fragment, whereas this fragment was expected to shift to 9.6 kb in case of a homologous integration of the deletion construct into the *mclA* locus. Transformants SMBA9 and SMBA10 exactly showed the expected pattern, whereas others seem to posses either tandem and/or ectopic integrations (Fig. 2).

Phenotypic characterization of methylisocitrate lyase deletion mutants. In order to study the phenotypes caused by a deletion of the *mclA* gene, growth experiments were performed on solid and liquid media. Liquid media were used to investigate a potential growth inhibitory effect by determination of the dried biomass, whereas solid agar plates were used to study the effect of propionate on asexual development. The effects of different carbon sources on development are illustrated in Fig. 3A. With propionate as the sole carbon and energy source the deletion strains did not produce any visible biomass or conidia, not even after incubation for more than 5 days. Therefore, we conclude that the methylisocitrate lyase is essential for the utilization of propionate. In contrast, no phenotype was visible, when glucose or acetate was used as sole carbon sources. This finding implies that methylisocitrate lyase is specifically involved in the methylcitrate cycle and not required for the citric acid or glyoxylate cycle. Addition of 20 mM propionate to glucose medium totally abolished the formation of conidia. However, a microscopic investigation of the colonies showed that development of conidiophores, including metulae and phialides was not disturbed (data not shown). Nevertheless, an extra addition of 50 mM acetate led to a slight restoration of conidiation. This is in agreement with the competition of acetate and propionate for the activation to the corresponding CoA ester as shown previously (5). Furthermore, when acetate was the main carbon source, propionate only showed a strong reduction of conidiation when used in the same or even in a higher concentration.

A strong negative effect on biomass formation caused by the addition of propionate was observed when strains were grown in liquid media. It has been shown that propionate possesses some inhibitory effect on growth of an *A. nidulans* wild-type strains when glucose was the main carbon source (7). A 40% reduction of biomass was observed when 50 mM propionate was added, and a 60% reduction was observed in the presence of 100 mM propionate. On the other hand, the addition of various amounts of propionate had no effect on biomass for-

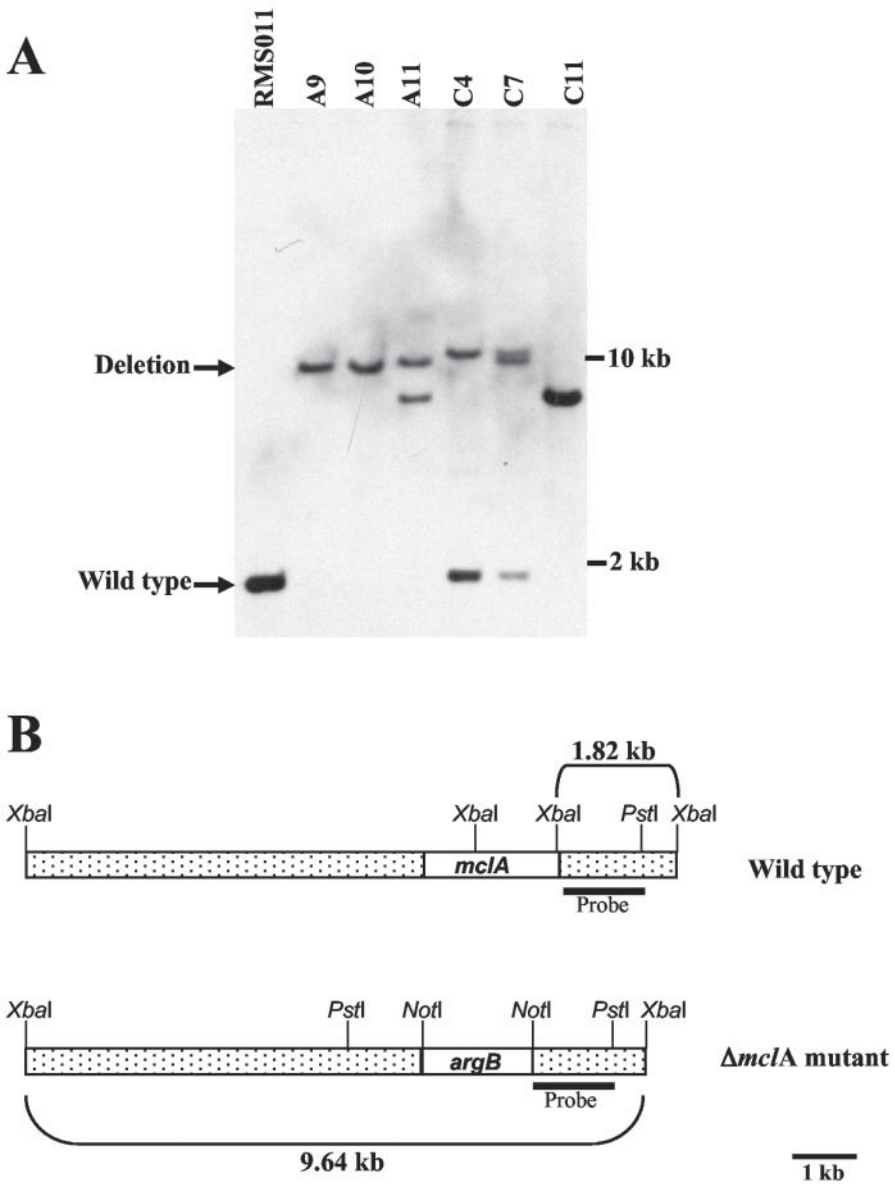

FIG. 2. Southern analysis of transformants. (A) Southern blot of different transformants in comparison to the original *mclA*$^+$ strain RMS011. Strains A9 and A10 show the expected shift from 1.8 to 9.6 kb. (B) Diagram of the wild type and a transformant with a homologous integration of the deletion construct.

mation when acetate was the main carbon source. Compared to that the methylisocitrate lyase mutants were severely affected in growth when glucose-propionate or acetate-propionate served as carbon sources. The strongest inhibitory effect was noticed when glycerol was the main carbon source (Table 2). This insinuates a severe inhibition of mitochondrial metabolism because glycerol is, like glucose, metabolized via the citric acid cycle without the gain of energy from cytoplasmic glycolysis.

Confirmation of mutant phenotype by sexual crossing. In order to confirm that the observed phenotypes were due to a deletion of the genomic locus coding for methylisocitrate lyase and were not caused by other secondary effects, the mutant strain SMBA9 was crossed with strain SRF200. The transformant strain SMBA9 was prototroph for arginine because the *argB* gene was used as a selection marker during transformation. Nevertheless, the original copy of *argB* in this strain was still deleted. Strain SRF200 also carried a deleted *argB* locus. Due to that constellation, all arginine prototrophic progenies of the sexual crossing were supposed to carry a deleted methylisocitrate lyase gene and should show a sporulation defect in the presence of propionate. Because of the different conidial colors of the two strains (yellow for SMBA9 and green for SRF200), ascospores deriving from a crossing event of the two partners were easily identified by the deviation of green and yellow spore color of the offsprings from a single cleistothecium. For crossing, the carbon source solely consisted of glucose. Under this condition, no phenotype in cleistothecia for-

DOCKET ALARM

Explore Litigation Insights

Docket Alarm provides insights to develop a more informed litigation strategy and the peace of mind of knowing you're on top of things.

Real-Time Litigation Alerts

Keep your litigation team up-to-date with **real-time alerts** and advanced team management tools built for the enterprise, all while greatly reducing PACER spend.

Our comprehensive service means we can handle Federal, State, and Administrative courts across the country.

Advanced Docket Research

With over 230 million records, Docket Alarm's cloud-native docket research platform finds what other services can't. Coverage includes Federal, State, plus PTAB, TTAB, ITC and NLRB decisions, all in one place.

Identify arguments that have been successful in the past with full text, pinpoint searching. Link to case law cited within any court document via Fastcase.

Analytics At Your Fingertips

Learn what happened the last time a particular judge, opposing counsel or company faced cases similar to yours.

Advanced out-of-the-box PTAB and TTAB analytics are always at your fingertips.

API

Docket Alarm offers a powerful API (application programming interface) to developers that want to integrate case filings into their apps.

LAW FIRMS
Build custom dashboards for your attorneys and clients with live data direct from the court.

Automate many repetitive legal tasks like conflict checks, document management, and marketing.

FINANCIAL INSTITUTIONS
Litigation and bankruptcy checks for companies and debtors.

E-DISCOVERY AND LEGAL VENDORS
Sync your system to PACER to automate legal marketing.